Chapter 3
Analysis and Implementation of an 84-Pulse STATCOM

Antonio Valderrabano-Gonzalez, Juan M. Ramirez, Ruben Tapia-Olvera, Julio C. Rosas-Caro, Jose M. Lozano-Garcia and Juan Miguel Gonzalez-Lopez

Abstract This chapter describes the use of STATCOM for the reactive power compensation and the power quality improvement. The assembling of a Voltage Source Converter (VSC) that meets the IEEE Recommended Practices and Requirements for Harmonic Control in Electrical Power Systems (IEEE Std. 519-1992) is emphasized. The low Total Harmonic Distortion (THD) that this VSC generates, qualifies this power conditioner to be considered for its use on stringent applications. The reinjection principle is used, that makes this proposal be considered as an affordable solution to the sinusoidal synthesis due to the reduced number of switches. The reinjection transformer is one of the most important elements in this configuration, and it can have a wide turn ratio variation without

A. Valderrabano-Gonzalez (✉) · J.C. Rosas-Caro
Universidad Panamericana Campus Guadalajara, Calz. Circ. Pte. No.49,
Cd. Granja, 45010 Zapopan, JAL, Mexico
e-mail: avalder@up.edu.mx

J.C. Rosas-Caro
e-mail: crosas@up.edu.mx

J.M. Ramirez
Centro de Investigacion y de Estudios Avanzados del Instituto Politecnico Nacional,
Av. del Bosque 1145, Col. el Bajio, 45019 Zapopan, JAL, Mexico
e-mail: jramirez@gdl.cinvestav.mx

R. Tapia-Olvera
Universidad Politecnica de Tulancingo, Calle Ingenierias No. 100. Col. Huapalcalco,
43629 Tulancingo, HGO, Mexico
e-mail: ruben.tapia@upt.edu.mx

J.M. Lozano-Garcia
Division de Ingenierias Campus Irapuato-Salamanca, Universidad de Guanajuato,
Carr. Salamanca—V. de Santiago, Comunidad de Palo Blanco, 36885 Salamanca,
GTO, Mexico
e-mail: jm.lozano@ugto.mx

J.M. Gonzalez-Lopez
Universidad Tecnologica de Manzanillo, Camino Hacia Las Humedades S/N,
Col. Salahua, 28869 Manzanillo, COL, Mexico
e-mail: jmgonzalez@utmanzanillo.edu.mx

F. Shahnia et al. (eds.), *Static Compensators (STATCOMs) in Power Systems*,
Power Systems, DOI 10.1007/978-981-287-281-4_3

leading out the special application standards. Conventional Proportional-Integral (PI) controllers are applied to hold the output voltage of the STATCOM around nominal conditions. The followed strategy employs the error and its variation to break down the control action into smaller sections that can be selected according to simple rules.

Keywords STATCOM · Multi-pulse · THD · Fuzzy segmented PI · VSC

3.1 Introduction

Deregulation, open access, and cogeneration in electrical power systems are creating transmission congestion scenarios and forced outages. Increasing the number of transmission lines is a non-viable solution to these potential problems, mainly due to costs and environmental issues. To have efficient and reliable power system operation, new control schemes are needed to be developed to handle dynamic disturbances such as transmission lines tripping, loss of generation, short-circuits, load rejection, while the reactive control has to be fast enough to maintain the desired voltage levels and the system stability. Flexible Alternating Current Transmission System (FACTS) devices have been proposed for fast dynamic control of voltage, impedance, and phase angle in high-voltage AC lines. The application of this technology has opened new and better opportunities for an appropriate transmission and distribution control. The series and shunt power systems compensation is used with the purpose of improving the operating conditions. Respect to the voltage, the compensation has the purpose of handling reactive power to maintain bus voltages close to their nominal values, reduce line currents, and reduce system losses. The voltage magnitude in some buses may be controlled through sophisticated and versatile devices such as the STATCOM, which can synthesize the reactive power from small values of storing elements [1], and is a power reactive source [2, 3]. By regulation of the STATCOM output voltage magnitude, the reactive power exchanged between the STATCOM and the transmission system can be controlled [4–8].

Since the STATCOM may cause interference on the system's fundamental sine wave at frequencies that are multiples of the fundamental one, special care should be paid to ensure preventing further harmonic problems. In general, there are three common strategies to construct a VSC while minimizing the harmonic content at the output: (i) the multi-pulse; (ii) the multilevel; (iii) and the Pulse-Width Modulation (PWM) [9, 10].

In the multi-pulse strategies, the period of the signal is broken down into equal sized parts with respect to the pulse number. Switches are triggered once per cycle at the fundamental frequency, and the pulse's amplitude is controlled mainly by the magnetic output stage. Higher number of pulses results in less output THD.

In the multilevel strategy, the DC source has to be broken down into parts of equal amplitude (x), resulting in a signal of $2x - 1$ levels. Switches are also switched once per cycle at the fundamental frequency. The output THD depends on the number of DC sources or divisions available in the DC link.

On the other hand, the PWM strategy uses fast commutations to obtain a low THD. The faster commutations are the lower THD; however, it is limited because of the commutation speed of the switches and requires always an output filter to be coupled to the grid.

This research deals with a combination of multi-pulse and multilevel strategies with emphasis on the use of multi-pulse configurations in order to reach the minimum THD.

Several methods has been investigated for stepping-up the number of pulses in the multi-pulse converter output. The simplest one is by increasing the number of 6-pulse modules through their corresponding transformers (four 6-pulse converters result in 24-pulse, eight 6-pulse converters result in 48-pulse operation, and so forth). The weakness of this method is the large size and high cost due to the number of bridges and transformers. Thus, in order to utilize the VSC in special applications such as airports or hospitals, to attain an 84-pulse signal, an array of fourteen 6-pulse modules with 42 transformers is required, besides a huge control task to have a reduced THD, which makes the entire array an impractical solution. A good strategy to get the 84-pulse waveform from a 12-pulse along with an eight level reinjection converter is presented in [9]. It has 26 extra switches and 7 DC voltage sources (capacitors) compared to the conventional 12-pulse converter. The control task is hard because of the number of gate signals needed, and it is prone to unbalance problems due to the large chain of capacitors. Multilevel Voltage Reinjection (MLVR) H-bridge conversion is another option to generate the 84-pulse signal. It requires 5 additional DC voltage sources and 12 switches compared to the conventional 12-pulse converter, but it can be easily used to have more levels in the reinjection by adding H-bridges in series [11]. An auxiliary multilevel circuit in the DC link side has been proposed for reinjection in [5–7, 10, 12]; it employs fewer components while the THD is bigger than that needed for special applications. This research presents a strategy to generate the 84-pulse VSC, assembled by combining one 12-pulse converter with one seven-level converter used as the reinjection scheme. The extra components, respect to the conventional 12-pulse converter, are: 8 switches, 4 DC voltage sources, 4 diodes for the seven-level converter, and one reinjection transformer. This amount of components and the wide turn ratio allowed by the reinjection transformer constitute an attractive array in terms of cost and reduced output voltage THD.

STATCOM is a FACTS device with a great deal of attributes, such as quick response in the adjustment of the required output levels, fewer space requirements than other shunt FACTS devices, flexibility, and excellent dynamic characteristics under various operating conditions. Its main objective is to generate an almost harmonic-free and controllable three-phase AC output voltage waveform at the Point of Common Coupling (PCC), to regulate reactive current flows by generating and absorbing controllable reactive power through the solid states switching

algorithm [13]. This is one of the most widespread devices studied. However, the state-of-the-art review indicates that a high number of switches, magnetic and reactive elements are needed in order to be able to get a low output THD. This research has been proposed taking into account the current technologies and the advantages of each one on the VSCs assembling, including the advantages of using the multilevel strategies on the synthesis of a staircase signal with a low number of reactive components, but with the low switching speed characteristic of the multi-pulse converters, and also a low number of magnetic devices. The proposed strategy saves the total amount of switching devices, while renders low THD, which is really attractive in special applications.

3.2 84-Pulses STATCOM

STATCOM is a power electronics-based Synchronous Voltage Generator (SVG) which is capable to provide fast and continuous capacitive and inductive reactive power supply. It generates a three-phase voltage, synchronized with the transmission voltage, from a DC energy source, and it is connected to the electric power system by a coupling transformer. The regulation of the STATCOM's output voltage magnitude gives rise to the reactive power exchange between the STATCOM and the transmission system. The STATCOM's basic structure, illustrated on Fig. 3.1, consists of a step-down transformer, a three-phase VSC, and a DC capacitor [2, 5, 6, 8, 14].

3.2.1 Reinjection Configuration

There are three main strategies to implement a VSC: (i) the multi-pulse; (ii) the multilevel; (iii) and the PWM [9, 10].

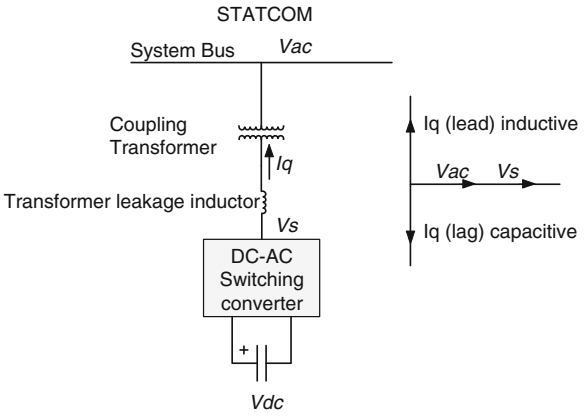

Fig. 3.1 STATCOM basic structure and V–I characteristic

There is a difference on the 12-pulse converter used in this research respect to the standard 12-pulse converter. The DC source is not common to both 6-pulse modules. In this proposition, a positive multi-pulse signal between the main terminals of the first 6-pulse converter and another positive multi-pulse signal with opposite phase between the main terminals of the second 6-pulse converter are connected. In order to have a neutral point, the negative terminal of the first converter is connected to the positive terminal of the second converter.

Each branch in the 6-pulse converters must generate electrical signals with 120° of displacement between them; the upper switch is conducting while the lower one is open and vice versa (180° voltage source operation) [15].

A 30° displacement in the firing sequence of both converters must be considered. Transformer turn ratios are 1:1 and 1:$\sqrt{3}$ on the YY and YΔ transformers, respectively. In order to operate the VSC in special applications such as airports or hospitals, an 84-level voltage signal is generated through a seven-level auxiliary circuit operating as a re-injection scheme. The auxiliary circuit is common to the three phases, reducing the number of extra components. The topology to provide the pulse multiplication is detailed in [9, 10, 12, 16–19], and illustrated in Fig. 3.2.

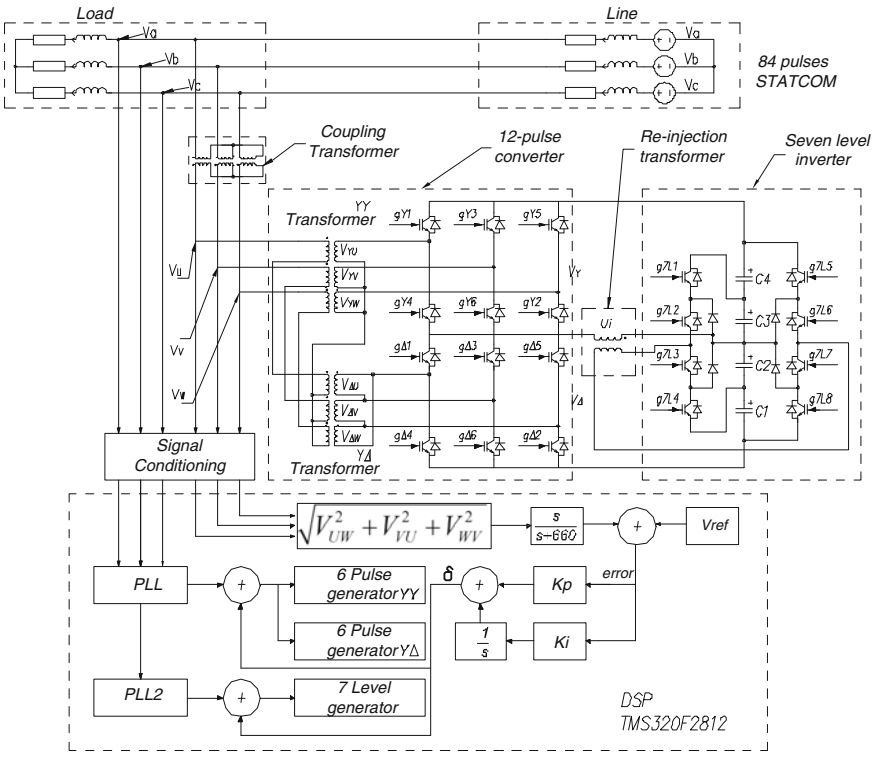

Fig. 3.2 84-pulse STATCOM structure

3.2.2 Total Harmonic Distortion

In order to apply the seven-level inverter output voltage to feed the standard 12-pulse converter, special care should be paid for not applying negative voltage into V_Y or V_Δ; notice the inclusion of the injection transformer between both arrays. Thus, input voltages in the 6-pulse converter may be regulated by adjusting the injection voltage U_i by:

$$V_Y = V_{DC} + U_i \tag{3.1}$$

$$V_\Delta = V_{DC} - U_i \tag{3.2}$$

The injection voltage is determined by the seven-level inverter switching pattern, and the injection transformer turns ratio. When voltages V_Y and V_Δ are used as inputs to the 6-pulse converters, less THD will appear at the output of the VSC. Figure 3.3 exhibits the followed strategy to generate V_{YU} and $V_{\Delta U}$ as the interaction of the seven-level output and the corresponding 6-pulse signals [20]. These signals have been obtained from an electrical simulation developed in PLECS®, within MATLAB/Simulink environment.

Using the 1:1 ratio in the YY transformer, and $1{:}\sqrt{3}$ for the YΔ transformer, adding their corresponding output signals in a series connection, the 84-pulses line-to-neutral signal VU emerges Fig. 3.4a, with the harmonic spectrum in Fig. 3.4b (linear scale) and in Fig. 3.4c (logarithmic scale).

The STATCOM's phase voltage VU is an odd symmetric signal, so that the even terms of the Fourier series become zero. Thus,

$$V_U(t) = \sum_{n=1}^{\infty} V_{U_{2n-1}} \sin((2n-1)\omega t) \tag{3.3}$$

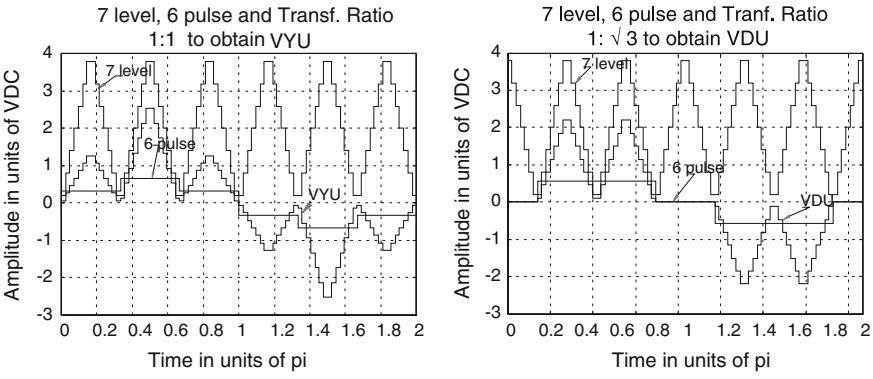

Fig. 3.3 Mixing seven-level, 6-pulse signals, and transformer ratios to attain V_{YU} and $V_{\Delta U}$

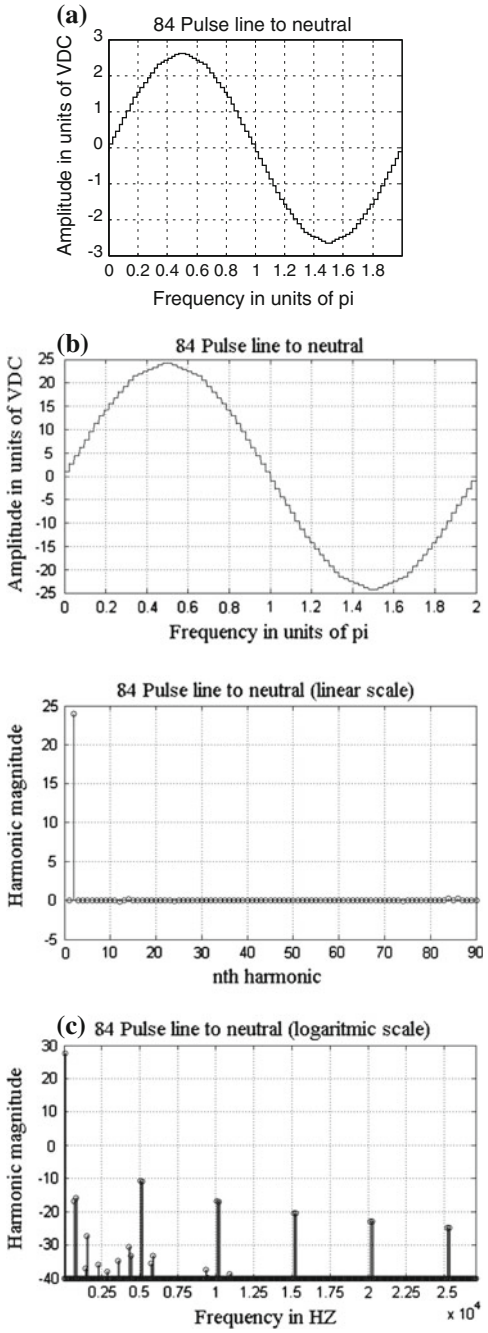

Fig. 3.4 **a** 84-pulses line-to-neutral output voltage, **b** 84-pulses harmonic content (linear scale), 84-pulses harmonic **c** content (logarithmic scale)

$$V_{U_{2n-1}} = \frac{4V}{3\pi(2n-1)}(A_{2n-1} + aB_{2n-1}) \tag{3.4}$$

$$A_{2n-1} = 2 + 2\cos\left(\frac{1}{3}\pi(2n-1)\right) + 2\sqrt{3}\cos\left(\frac{1}{6}\pi(2n-1)\right) \tag{3.5}$$

$$B_{2n-1} = \sum_{i=0}^{20} Coeff_i \cos\left(\frac{i}{42}\pi(2n-1)\right) \tag{3.6}$$

$$Coeff = \begin{Bmatrix} -3, & 1, & 1, & 1, & 1, & 1, & 1, \ldots \\ -3\sqrt{3}, & \sqrt{3}-1, & \sqrt{3}-1, & \sqrt{3}-1, & \sqrt{3}-1, & \sqrt{3}-1, & \sqrt{3}-1, \ldots \\ -3, & -\sqrt{3}+2, & -\sqrt{3}+2, & -\sqrt{3}+2, & -\sqrt{3}+2, & -\sqrt{3}+2, & -\sqrt{3}+2 \end{Bmatrix} \tag{3.7}$$

assuming that a is the turns ratio of the re-injection transformer.

The 84-pulse signal value (VU) depends on a which is determined in order to minimize the THD, defined by [10, 21]

$$THD_{VU} = \sqrt{\frac{\sum_{n=2}^{\infty} V_{Un}^2}{V_{U1}^2}} \tag{3.8}$$

The minimization of THD yields the parameter a. In this research, calculation has been carried out in MATLAB with n = 7,200, and increments of $\Delta a = 0.0001$. With these parameters, the minimum THD becomes 2.358 % with $a = 0.5609$, value used on the previous figures.

The distortion limits according to the IEEE Std. 519 indicate that the allowed THD in voltage is 10 % in dedicated systems, 5 % in general systems, and 3 % for special applications as hospitals and airports [21].

Table 3.1 presents the minimum THD in the output voltage produced with several multi-pulse configurations. The THD produced through this proposition allows its use even in applications with stringent quality requirements; it exhibits less dependence to variations on a, which can have variations until ±12 % to get a maximum THD lower than 3 %. This means that a strict reinjection transformer's turn ratio is not needed to get a THD within a stringent condition. Figure 3.5

Table 3.1 Minimum THD produced through the multi-pulse VSC

Number of pulses	THD (%)
12	15.22
24	7.38
48	3.8
60	3.159
84	2.358

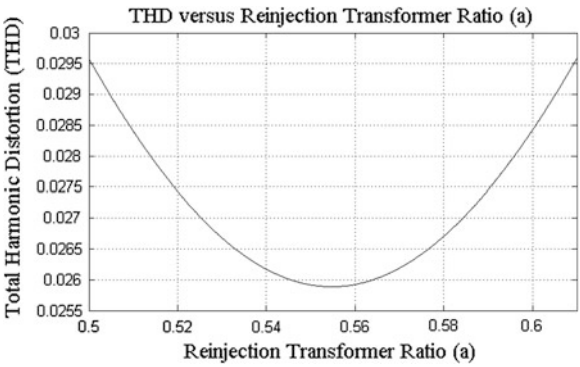

Fig. 3.5 Dependence of the THD respect to the turn ratio of the reinjection transformer

illustrates the dependence of the THD respect to variations in the re-injection transformer turn ratio a. All these values had been obtained using MATLAB.

3.2.3 STATCOM Arrangement

In order to connect the improved VSC to the system for reactive compensation, several points have to be taken into account. This section deals with those details using Fig. 3.2 as the main scheme, including a coupling transformer 13.8:13.8 kV, and considering the following transmission line parameters, at 75° C:

- Conductor code name: Grosbeak Aluminum Conductor Composite Core (ACCC)
- Voltage rating: 13.8 kV peak
- Resistance: 0.0839 Ω/km
- Inductive Reactance: 0.2574 Ω/km
- Line length: 50 km
- Load Resistance: 202.5 Ω
- Load Inductive Reactance: 0.6 H

If we pursue to eliminate the active power exchange between the STATCOM and the system, the DC voltage sources are replaced by capacitors.

Secondly, it must be ensured that the frequency and phase angle at the output of the STATCOM are equal to the system ones; these parameters will be obtained by a synchronizing arrangement which is able to detect instantaneously the phase angle. The seven-level inverter must switch at six times the frequency of the 6-pulse converters to ensure phase and frequency.

The digital signal processor (DSP)-control implementation must take the voltage levels needed for the Analog to Digital Converters (ADC) to detect the signals with appropriate precision, and must refresh the output data before taking new samples to be considered real time. It is also needed to provide isolation from the power stage.

3.2.4 Phase-Locked-Loop

The Phase-Locked Loop (PLL) is the synchronizing circuit responsible for the determination of the system frequency and phase-angle from the fundamental positive sequence voltage of the controlled AC bus [22]. The PLL utilizes the Stationary Reference Frame (SRF) in order to reduce computational costs, and helps to improve the system dynamic performance [23]. Digital PLL is an algorithm which can detect the fundamental component of the phase-voltages to synchronize the output signal to the frequency and phase of the input one. This algorithm does not require a zero crossing detection routine for the input voltage or the generation of internal reference signals for the input current [24]. The proposed PLL strategy employs a—$\tan^{-1}(\alpha/\beta)$ function added to a correction value determined by the signs of α and β, as shown in Fig. 3.6a. This block synchronizes the zero output of the PLL with respect to the startup signal α, when signal β attains its minimum value as shown in Fig. 3.6b.

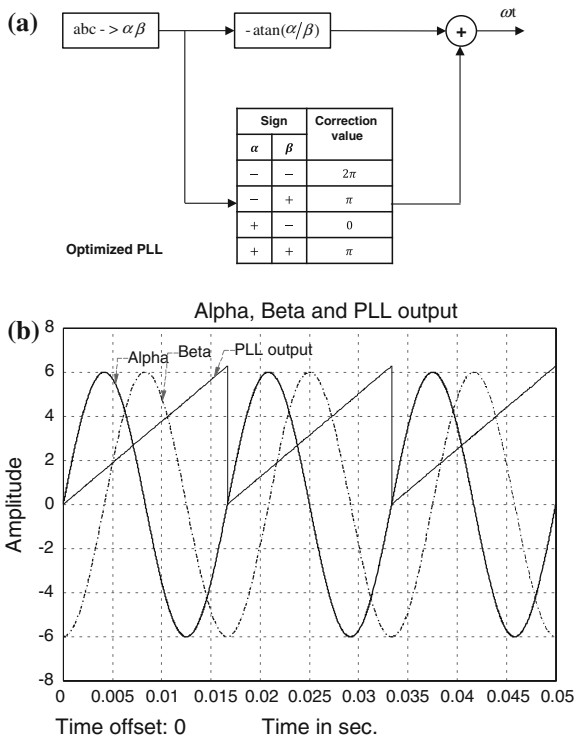

Fig. 3.6 **a** PLL strategy, **b** α, β, and PLL-output

3.2.5 Firing Sequence

The second block is the 6-pulse generator, which is responsible for generating the pulse sequence to fire the three-phase IGBT arrays. It consists of an array of 6-pulse spaced 60° from each other. In this block, the IGBT will operate at full 180° for the *on* period and 180° for the *off* period. Any disturbance in the frequency will be captured by the synchronizing block, preventing errors. The falling border in the synchronizing block output signal is added to a series of six 60° spaced signals that would be sent to the opto-coupler block gate, which will feed each 6-pulse converter. The off sequence turns off in a similar way but waiting 180° to keep the same duration *on* and *off* for each IGBT.

3.2.6 Seven-Level Generator

In order to produce the pulse sequence needed to generate the seven-level inverter, six times the frequency of the 6-pulse generator should be ensured beginning at the same time. This is achieved by monitoring the falling border in the novel PLL output signal, and using it along with the modulus operator with the π/3 argument. This signal will be the period for the seven-level generator, which will modify its state every π/42 rad. Figure 3.7 depicts the asymmetric pulse sequence for such seven-level inverter, along with the voltage for a complete sinusoidal cycle and a π/3 zoom-in, in order to observe the detailed pulse signals.

3.2.7 Angle Control Circuit

The reactive power exchange between the AC system and the compensator is controlled by varying the fundamental component magnitude of the inverter voltage,

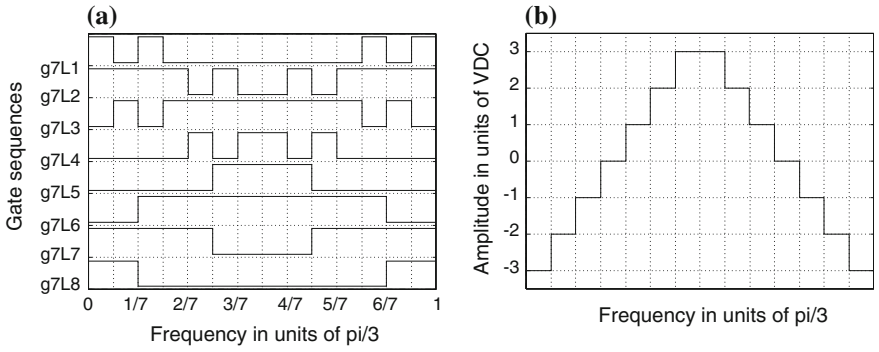

Fig. 3.7 Seven-level gate signals and output. **a** Gate sequence 7 level converter. **b** Output signal 7 level converter

above and below the AC system level. The compensator control is achieved by small variations in the switching angle of the semiconductor devices, so that the first harmonic component of the voltage generated by the inverter is forced to lag or lead the AC system voltage by a few degrees. This causes active power to flow into or out of the inverter, modifying the value of the DC capacitor voltage, and consequently. Subsequently, this will affect the magnitude of the inverter terminal voltage and the resultant reactive power [5]. The angle control block diagram is described in [23] for a PI controller, and depicted in Fig. 3.8.

The inputs are the line-to-line voltages of the controlled AC bus prior to the coupling transformer. The reference voltage VREF is chosen as the RMS value for a pure sinusoidal three-phase signal, which is $\sqrt{1.5}$ times the peak of the line voltage. This value is compared to the filtered RMS voltage at the output of the STATCOM (VRMS) multiplied by the turn ratio of the coupling transformer. The output signal δ corresponds to the displacement angle of the generated multi-pulse voltages, with respect to the controlled AC bus voltage (primary voltage of the converter transformer). The Low Pass Filter (LPF) is tuned to remove the characteristic harmonic content in the multi-pulse configurations; for the 12-pulse and begins with the 11th harmonic. The PI controller has a limiting factor by dividing the error signal by the reference voltage V_{REF} in order to have the δ signal with a maximum value of –1 when the STATCOM output is equal to zero.

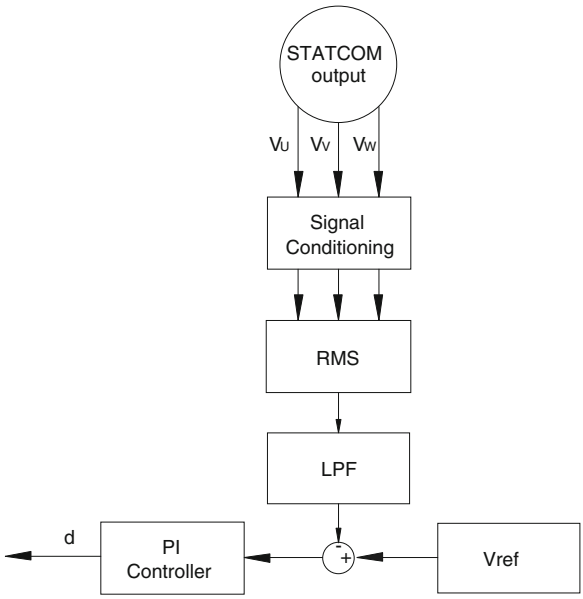

Fig. 3.8 STATCOM power angle control

3.3 Control Strategy

Conventional PI or Proportional-Integral-Derivative (PID) regulators have been applied to control the STATCOM output voltage under nominal and dynamic conditions [25–28]. Such controllers may exhibit poor performance when the error signal jumps with big steps in magnitude. It is desirable to find a controller that can deal with most of the problems detailed in [29]. The strategy followed employs the error and error variation to break down the control action in smaller sections that can be selected according to simple rules [30].

3.3.1 Segmented PI Controller

The complete system presented on Fig. 3.2 was tested under several disturbances using a PI controller tuned for steady state operation. Special attention is paid to measure the error and estimate the error increment when the disturbances are applied. It is verified that a motor startup is a quite demanding situation to test the STATCOM performance, so it was used to define the membership function limits. For simplicity on the controller design, crisp membership functions were used to describe seven linguistic variables similarly to the fuzzy set notation as follows:

- NB → negative big,
- NM → negative medium,
- NS → negative small,
- Z → zero,
- PS → positive small,
- PM → positive medium,
- PB → positive big.

Figure 3.9a displays the error signal, which has a range from −1 to +1, and Fig. 3.9b exhibits the variation of this error. This parameter is estimated using MATLAB ode23t solver with a variable step. The error (E) and its variation (DE) are represented by lowercase as the independent variables; they are continuous values. The uppercase represents the fuzzy set obtained by selecting the indicated membership functions' limits.

Fuzzy control rules are usually obtained empirically. This chapter uses the rules presented in [31] to define the zones of the segmented PI, Table 3.2.

The strategy to tune the segmented PI zones is summarized in the following steps.

1. Tune up a conventional PI at steady state. The proportional and integral gains obtained are: K_P = 0.5411, and K_I = 20.3718. Such values are used on the segmented PI controller as the initial conditions, preserving the same gain values in the seven zones. Thus, originally, the conventional PI and the segmented PI controllers are equivalent.

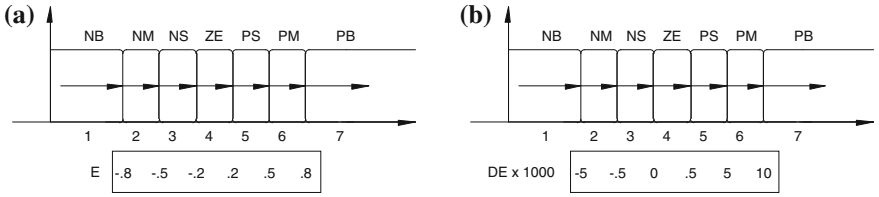

$$E = \begin{cases} \text{NB} & -\infty < e \le -.8 \\ \text{NM} & -.8 < e \le -.5 \\ \text{NS} & -.5 < e \le -.2 \\ \text{ZE} & -.2 < e \le .2 \\ \text{PS} & .2 < e \le .5 \\ \text{PM} & .5 < e \le .8 \\ \text{PB} & .8 < e \le \infty \end{cases} \qquad DE \times 1000 = \begin{cases} \text{NB} & -\infty < de \le -5 \\ \text{NM} & -5 < de \le -.5 \\ \text{NS} & -.5 < de \le 0 \\ \text{ZE} & 0 < de \le .5 \\ \text{PS} & .5 < de \le 5 \\ \text{PM} & 5 < de \le 10 \\ \text{PB} & 10 < de \le \infty \end{cases}$$

Fig. 3.9 Membership functions

Table 3.2 Control rules

E\DE	NB	NM	NS	ZE	PS	PM	PB
NB	1	1	1	2	3	3	4
NM	1	2	2	2	3	4	5
NS	1	2	3	3	4	5	6
ZE	1	2	3	4	5	6	7
PS	2	3	4	5	5	6	7
PM	3	4	5	6	6	6	7
PB	4	5	6	7	7	7	7

2. Taking into account that capacitors are used in the DC link in order to the system operates as STATCOM, and considering them fully discharged, we get a maximum error of −3. It is convenient to adjust the gains' value zone 1 due to it corresponds to the biggest negative error and the biggest negative error variation. To adjust the values of this zone, we must maintain K_P as low as possible to keep the system stable. Then, reduce K_I to the value that allows less oscillation in the segmented PI sections. After this step, zone 1 would have the values for the biggest negative error and error variation, while the remaining zones exhibit the original steady state values.
3. Starting up an induction motor when the capacitors are fully charged is considered one of the most demanding situations and is used for adjusting the remaining zones. To tune the gains of segment 2, use the value of K_P as low as possible to keep the system stable. Then, reduce K_I to the value that allows less oscillation in the zones presented on the right and low corner of Fig. 3.10, which will be discussed later.

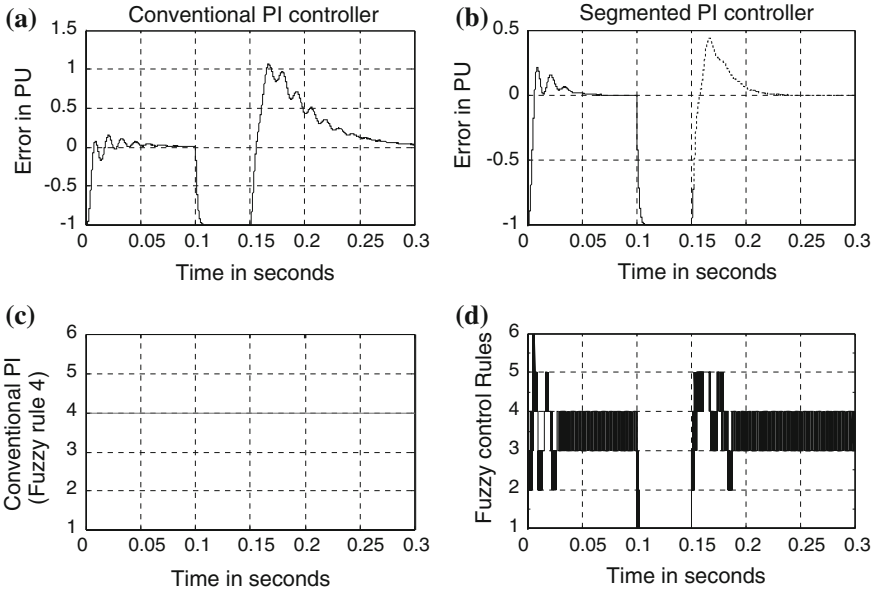

Fig. 3.10 Three-phase fault

Table 3.3 Gain values of the segmented PI

Fuzzy rule	K_P	K_I
1	0.5252	5.0929
2	0.5411	38.9929
3	0.5570	40.7436
4	0.5729	40.7436
5	0.5570	20.3718
6	0.4933	20.3718
7	0.3183	40.7436

4. Repeat step 3 for sections 3, 5, 6, and 7 in sequence. This will bring up to the segmented PI, Table 3.3. After tuning up the seven zones, the output will be between zones 3 and 4 on steady state.

It is important to note that using a different disturbance in the load or the source, the values would vary slightly, but the motor startup after getting to steady state (full capacitors charge) is the most demanding condition. Thus, using these values for tuning the segmented PI the controller will give good results for the most common power problems, such as Sags, Swells, etc.

3.3.2 Study Case

The STATCOM model and the segmented PI controller with the values obtained from the previous section were simulated in MATLAB/Simulink, using PLECS. PLECS is used because it is a fast simulation toolbox for electrical circuits within the Simulink environment specially designed for power electronics systems. It is also a powerful tool for any combined simulation of electrical circuits and controls. The PLL-block feeds the two 6-pulse generators at the fundamental frequency, and it is used to bring forth the seven-level pulses at six times the fundamental frequency to have them synchronized to the system and configured as the 84-pulse STATCOM. The δ signal calculated from the segmented PI controller is utilized to lag or lead the STATCOM voltage respect to the system. While the phase-angle lags the bus voltage ($\delta < 0$), energy is flowing to the DC capacitor, charging it and doing the STATCOM draws capacitive current. Contrarily, inductive current is drawn while ($\delta > 0$) [22].

The main advantages of this controller can be summarized with the system response to an interruption and a motor startup [30].

An interruption occurs when the supply voltage or load current decreases to less than 0.1 pu for a period of time not exceeding one minute. Interruptions can be the result of power system faults, equipment or control failures. An interruption, whether it is instantaneous, momentary, temporary, or sustained, can cause disruption, damage, and it can cause equipment failure, ruination of product, as well as the cost associated with downtime, cleanup, and restart [29, 32]. Figure 3.10 illustrates the controller error behavior after a 3-cycle three-phase fault at the load bus. The error is defined as the difference between the measured voltage and the reference voltage; the greatest error becomes −1 while the fault is on, but, once this one is released; the error is bigger than 1 pu with a conventional PI, as shown in Fig. 3.10a. In contrast, the segmented PI presents an error around 0.4 pu, as shown in Fig. 3.10b. The oscillations in the conventional PI response are smoothed with the use of the segmented controller. Figure 3.10c and d respectively illustrate rule number 4 for the conventional PI controller, and the rules of the segmented PI.

Oscillatory transients and voltage fluctuation commonly arise when a motor is connected. At this point, a sudden change in the steady-state condition of a signal's voltage, current, or both is performed and a series of random changes in magnitude and frequency is presented. A single PI is not as fast as needed to get a smooth startup. Figure 3.11 details the behavior of the error when a motor load is started.

The parameters of the induction motor are as follows:

- 2 250HP (2,300 V),
- Rs = 0.029 Ω,
- Lls = 0.0006 H
- Rr = 0.022 Ω,
- Llr = 0.0006 H,
- Lm = 0.0346 H,
- J = 6.5107 J.

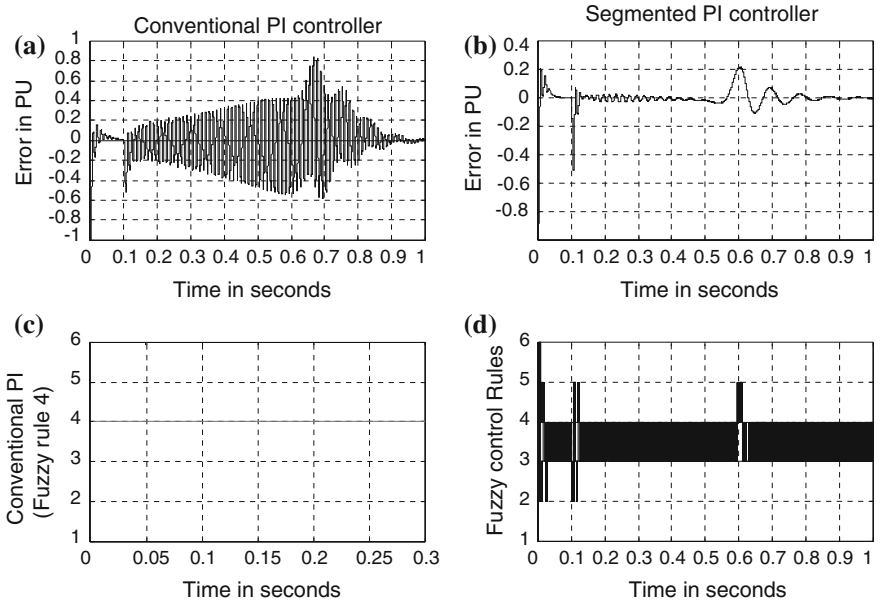

Fig. 3.11 Motor start up

The error signal, for the conventional PI exhibits several big oscillations as shown in Fig. 3.11a, while the segmented one exhibits very fast response to reach the steady state, and minimum oscillation as shown in Fig. 3.11b. Figure 3.13c, d are also included to illustrate the rule number 4 (conventional PI controller), and the rules of the segmented PI, respectively.

With these simulations it is demonstrated that when the system is stressed, the segmented PI controller presents an appropriate response.

3.4 Experimental Results

Previous sections have described the VSC structure as a STATCOM with the controller configuration. This section includes the results gotten on the experimental prototype built to verify the strategy, and are displayed through images coming from an oscilloscope for validation of each part of the device. These experimental results are exhibited as they were collected from the prototype, by increasing the complexity of the whole circuit. Important is to consider the nomenclature used, variables with subscripts a, b, or c, represent the source side, while variables with subscripts U, V, or W, are for the STATCOM output. When it is needed to differentiate both sides on the transmission line, subscripts a, b, or c are used, indicating if the source bus or the load bus is referred [33].

3.4.1 VSC Based on Multi-pulse Strategy

All the images presented in this section are captured with a Tektronix® TDS2024B oscilloscope which has only one reference point for the four acquired signals. Figure 3.12a, reveals the line-to-line voltage V_{UV} and V_{UW} of a 12-pulse VSC output (without connection to the grid), and illustrates that the 12-pulse converter output modified, exhibits exactly the same characteristics of a conventional 12-pulse converter when both input voltages (V_Y and V_Δ) of equal magnitude are used. Figure 3.12b, presents the single-phase seven-level inverter output (U_i) in (3.1) and (3.2) that is the needed signal at the input of the reinjection transformer. This signal has six times the system frequency, which is needed to have a complete cycle for each pulse on the 6-pulse converters output. The zero crossing of this signal must match with each three-phase zero-crossing.

In order to validate the strategy to build V_{YU} and $V_{\Delta U}$, Fig. 3.3 is used as a reference. The seven-level converter output, presented in Fig. 3.12b, is passed through the reinjection transformer connected as a step-down transformer; the transformer output U_i is added to the voltage of capacitors C4 and C3 to build V_Y,

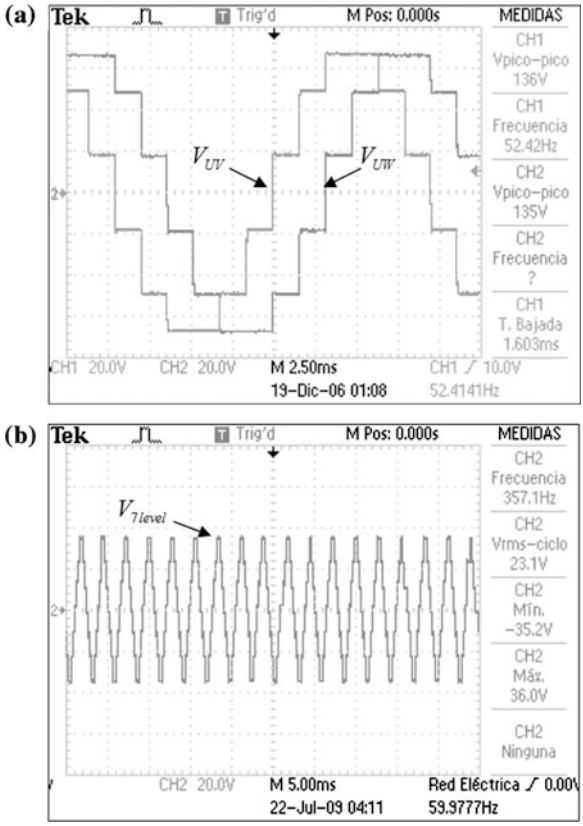

Fig. 3.12 **a** Conventional 12-pulse output voltages, **b** seven-level converter output

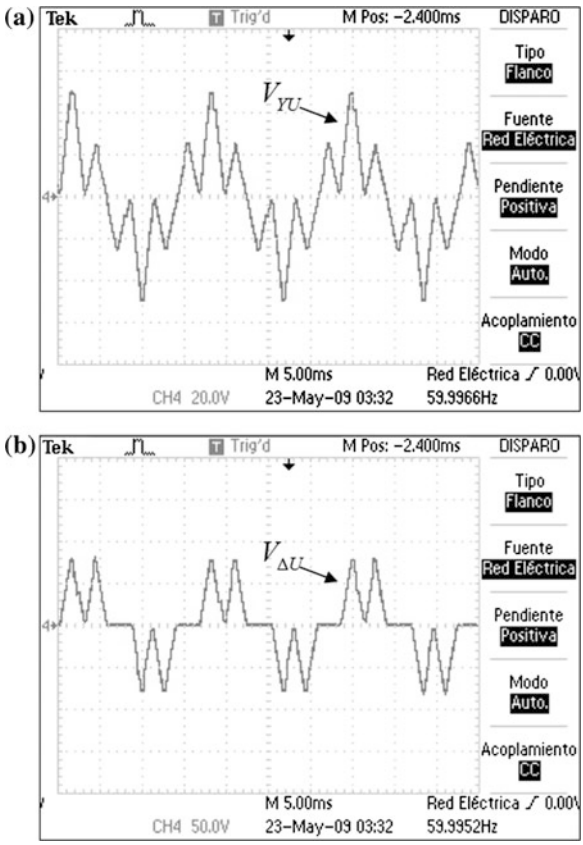

Fig. 3.13 **a** VYU built when the seven-level signal is injected into the 6-pulses converter with (YY-transformer), **b** VΔU built when the seven-level signal is injected into the 6-pulses converter (YΔ-transformer)

and C2 and C1 to build V_{Δ}. Voltage V_{DC}, corresponds to the voltage in capacitors C4 and C3, or C2 and C3. Using voltages V_Y and V_{Δ} as the inputs to the 6-pulse converters, and measuring after transformers YY and YΔ, the VSC outputs are those displayed in Fig. 3.13a, b. These signals have good agreement to the ones illustrated in Fig. 3.3.

Figure 3.14a verifies that by adding the voltages in Fig. 3.13a, b, the resultant waveform has the desired shape. The harmonic content is presented in Fig. 3.14b. It is attained by the Tektronix® TDS2024B oscilloscope. There are significant magnitude harmonics each about 5 kHz, which corresponds to the number $84r \pm 1$ $r = 0, 1, 2, \ldots$ when we use a 60 Hz signal. These harmonics are concurrent to the traditional multi-pulse harmonic content.

3.4.2 STATCOM Synchronized to the Grid

The PLL is the element responsible to determine the system frequency and the fundamental signal phase-angle. In order to verify its usefulness, Fig. 3.15a depicts

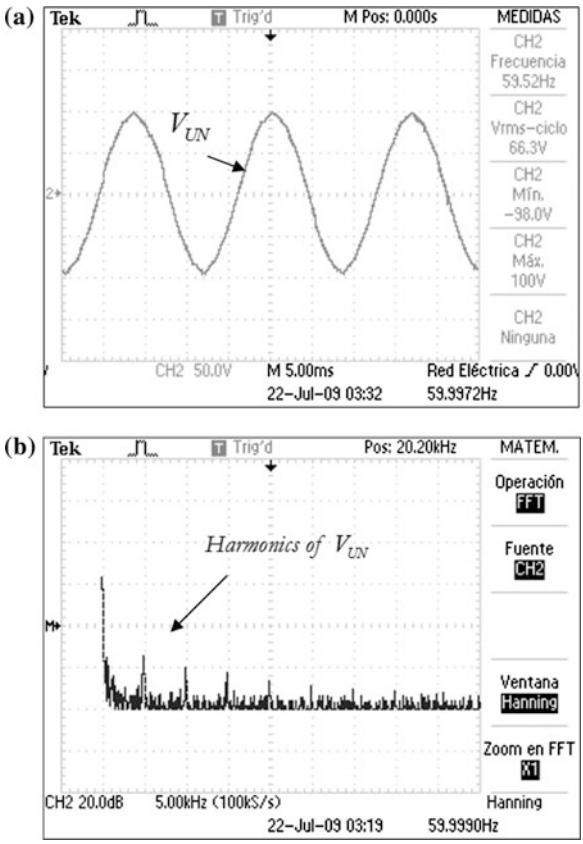

Fig. 3.14 **a** 84-pulses signal obtained through the combination of V_{YU} and $V_{\Delta U}$, **b** 84-pulses output signal harmonic content

the line voltage output of the VSC with respect to the grid line voltage. The waveform, phase, and output frequency, demonstrate the system ability to track the input, and the PLL effectiveness. Figure 3.15b displays the three-phase line-to-line voltages arisen from the VSC. It can be noticed that the angle difference among phases is 120°, as needed in a three-phase signal. The frequency of these signals is equal to that of the grid.

3.4.3 STATCOM Based on Energy Storage and Capacitors on the DC-Link

The use of an energy storage device, such as a bank of batteries, becomes quite important to verify the system behavior in the case of using DC renewable sources or battery storage to provide active power capabilities to the system [34–37]. However, due to the use of the DC source some effects that must be taken into account arise. They are summarized in this section.

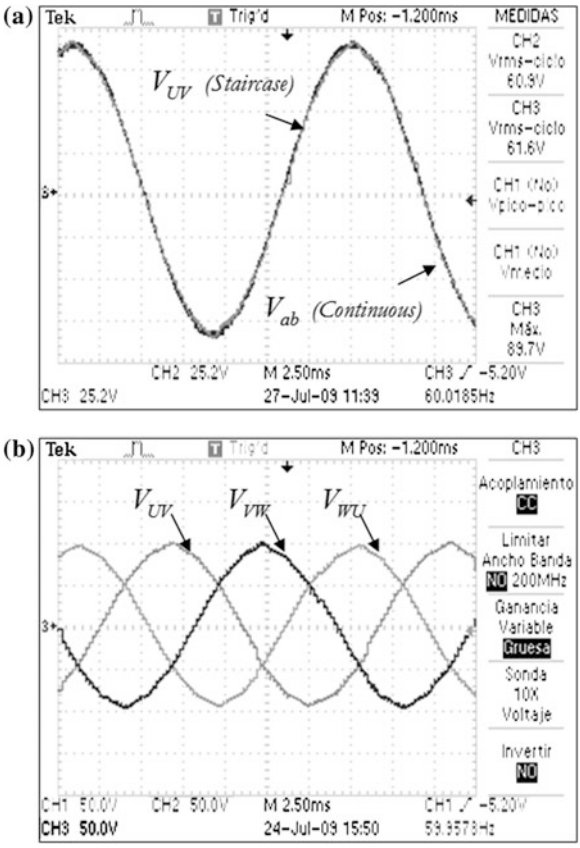

Fig. 3.15 **a** VSC output voltage synchronized in phase, frequency, and amplitude, **b** three phase 84-pulses VSC output

3.4.3.1 Notching

If a conventional 12-pulse STATCOM is used, the resulting voltage signal presents small disturbances in each pulse level change; these disturbances are termed notching [29]. The allowed notching limit according to the IEEE Std. 519 in special applications as hospitals and airports is 10 % [21]. This limit is exceeded by using a 12-pulse converter, especially around the zero crossing, Fig. 3.16a. The notching effect can be considerably reduced if the amount of pulses per cycle is increased. Figure 3.16b illustrates the reduced effect of notching when the 84-pulses STATCOM based on energy storage is employed.

3.4.3.2 Harmonics

The following figures are captured when the STATCOM based on energy storage is synchronized and connected to the grid. They illustrate one phase of the system, assuming that the behavior is similar in the two remaining phases.

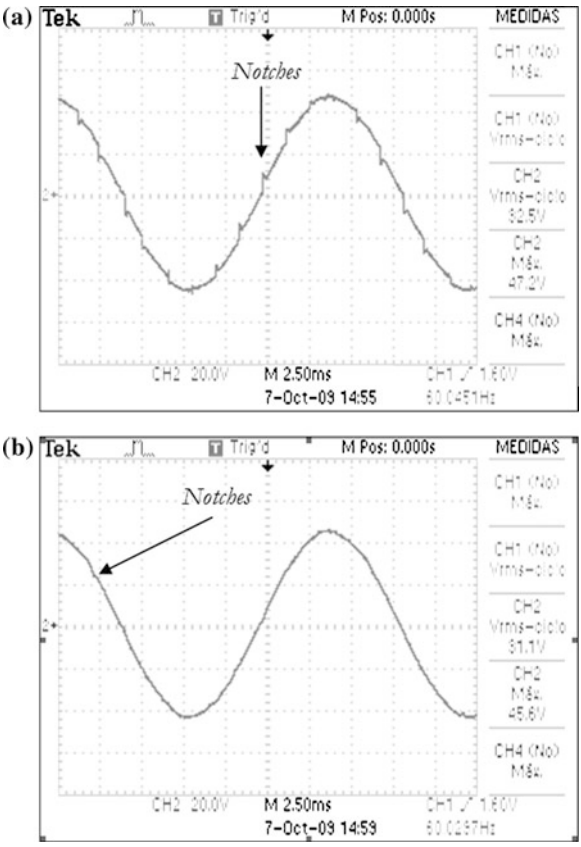

Fig. 3.16 **a** Notching produced by the 12-pulses STATCOM based on energy source, **b** the presence of notching is reduced by the 84-pulses STATCOM with energy source

Harmonic distortion is the pollution of the fundamental sine wave at frequencies that are multiples of the fundamental. Figure 3.17a depicts the phase voltage V_{aDSP} passed through the signal conditioning board, which is fed into the eZdsp TMS320F2812. This voltage is responsible of the synchronization. The VSC output, prior to the coupling transformer is also included and named as $V_U(STATCOM)$. The load voltage is presented as $V_a(Load)$ which has a magnitude of twice of the $V_U(STATCOM)$. These three signals have the same phase and frequency as the power system requires. The Fourier spectrum of $V_a(Load)$, when the STATCOM is not connected to the grid, is illustrated in Fig. 3.17b. The spectrum is calculated in the Tektronix® TPS2024 oscilloscope. Figure 3.17c depicts the spectrum of $V_a(Load)$ when the STATCOM based on energy storage is connected to the grid. In this case, small amplitude harmonics are repeated each 5 kHz.

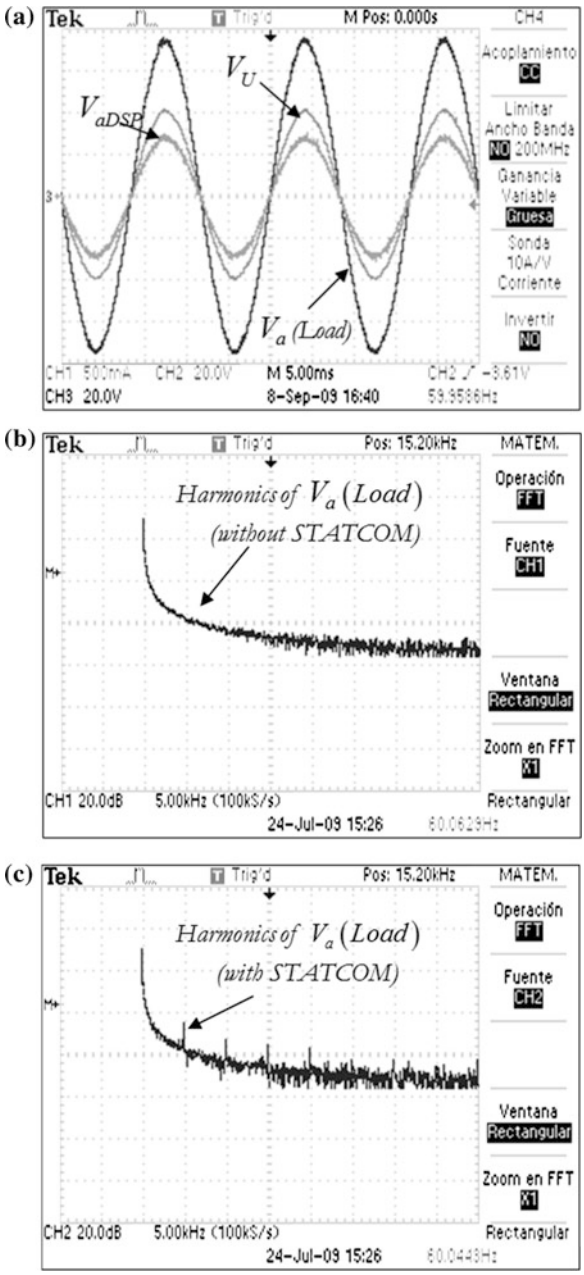

Fig. 3.17 **a** Voltage a fed into the DSP(V_{aDSP}), STATCOM output voltage (V_U), and load voltage of phase-a ($V_a(Load)$), **b** load voltage Fourier spectrum without STATCOM, **c** load voltage Fourier spectrum with the STATCOM based on energy source

3.4.4 STATCOM Reference Voltage Tracking Through a PI Controller

Once the STATCOM is connected to the grid, it is important to include a controller to verify its performance under some common variations. The STATCOM main objective is to maintain the voltage level on the load bus. Thus, the controller reference voltage is the magnitude of the voltage needed on the load, and has to be compared with the measured magnitude. A detailed explanation of the STATCOM operation is found at [8]. Referring to Fig. 3.2, the δ signal used on the pulse generators inside the DSP TMS320F2812 block, represents the phase displacement between the STATCOM and the grid. It is responsible for increasing or decreasing the STATCOM voltage. Through the appropriate δ selection, a conventional proportional-integral controller has been chosen and configured to have a losses' steady state compensation due to the transmission line parameters. This PI controller has been assembled in the DSP TMS320F2812 using the bilinear transformation to validate its behavior. Figure 3.18a shows voltage $V_a(Source)$ and voltage $V_a(Load)$ for the cases of low reference voltage. In this case, $V_a(Load)$ has the frequency and phase-angle corresponding to the $V_a(Source)$, but smaller magnitude. Capacitors were utilized for energy storage. Figure 3.18b depicts the case with nominal reference voltage. In this case, the $V_a(Load)$ has the frequency, the phase-angle, and the amplitude of the $V_a(Load)$, illustrating that the PI controller is able to command the line losses. This is the STATCOM normal operating condition in steady state. Figure 3.18c illustrates the case of high reference voltage. It is noticeable that the load voltage can be adjusted to that of the corresponding reference, although the influence of the 12-pulse converter becomes more evident when V_{ref} is higher than V_{source}. A more robust controller is needed to appropriately respond to commands in load higher voltage. The segmented PI controller proposed on this research demonstrates, via simulation, its ability to track low/high reference voltage.

3.4.5 Load Imbalance

Several researches have been made in order to use the STATCOM for source or load imbalance compensation [27, 38, 39]. Figure 3.19a displays some signals when a resistive load is used; phase-B in the load is in open-circuit to give rise to a load imbalance. The STATCOM is disconnected. Signal $V_a(Source)$ is phase-a voltage. Signal $V_a(Load)$ is the load voltage. It is worth noting the difference in amplitude and phase. The load current is in-phase with the load voltage due to the resistive load. Signal $P_a(Load)$ represents the instantaneous power on the load. Figure 3.19b demonstrates the usefulness of connecting a STATCOM based on

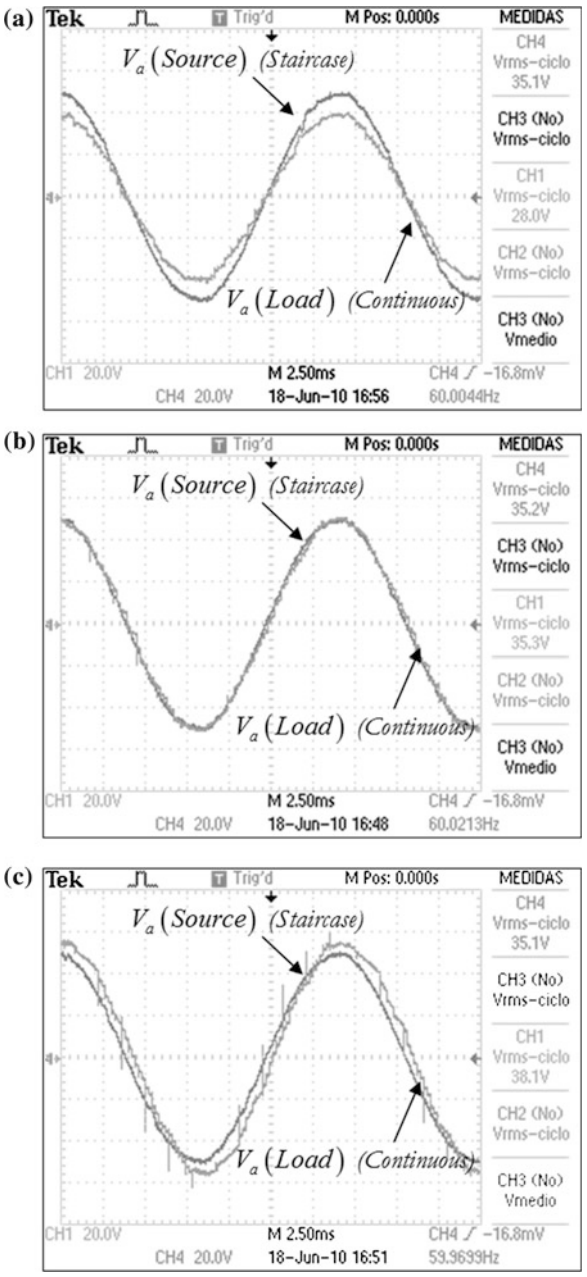

Fig. 3.18 **a** Load voltage when the reference voltage is lower than the source voltage, **b** load voltage when the reference voltage is equal to the source voltage, **c** load voltage when the reference voltage is equal to the source voltage

energy storage to the previous system. Signal $V_a(Source)$ is the phase-a voltage. Signal $V_a(Load)$ is the load voltage. Their overlapping is due to their same magnitude and phase. The load current $I_a(Load)$ becomes in phase with the load

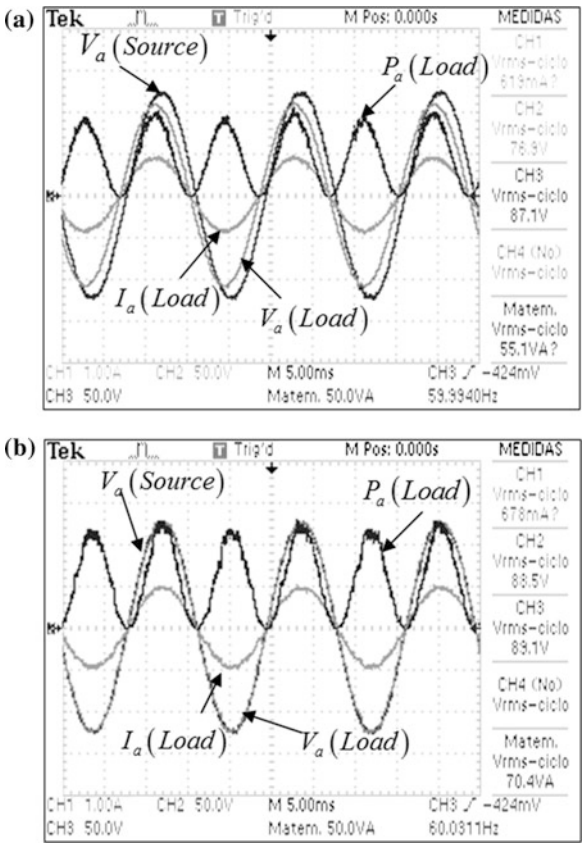

Fig. 3.19 **a** System with resistive load and STATCOM disconnected. **b** system with resistive load and the STATCOM based on energy storage

voltage, as a consequence of the resistive load. The $P_a(Load)$ signal represents the instantaneous power drawn in the load. A bigger power sent to the load is evident. The STATCOM is not designed to deal with unbalanced conditions. Using energy storage, active power can be used to solve unbalancing problems. Such condition needs separate controllers for each STATCOM phase.

References

1. Hingorani NG (2007) FACTS technology—state of the art, current challenges and the future prospects. In: Power engineering society general meeting, IEEE, pp 1–4
2. Song Y-H, Johns A (1999) Flexible ac transmission systems (FACTS). IET, Stevenage
3. Acha E, Fuerte-Esquivel CR, Ambriz-Perez H, Angeles-Camacho C (2004) FACTS: modelling and simulation in power networks. Wiley, New Jersey
4. Wang H (2000) Applications of damping torque analysis to STATCOM control. Int J Electr Power Energy Syst 22:197–204

5. Davalos-Marin R (2003) Detailed analysis of a multi-pulse StatCom. In: Cinvestav–internal report, May 2003. Available at http://www.gdl.cinvestav.mx/jramirez/doctos/doctorado/Predoctoral.pdf
6. El-Moursi M, Sharaf A (2005) Novel controllers for the 48-pulse VSC STATCOM and SSSC for voltage regulation and reactive power compensation. Power Syst IEEE Trans 20:1985–1997
7. Hingorani NG, Gyugyi L (2000) Understanding facts. IEEE press, New Jersey
8. CIGRE, Static Synchronous Compensator (1998) Working group 14.19 in Sept 1998
9. Liu Y, Arrillaga J, Watson N (2004) A new STATCOM configuration using multi-level DC voltage reinjection for high power application. Power Deliv IEEE Trans 19:1828–1834
10. Pan W, Xu Z, Zhang J (2007) Novel configuration of 60-pulse voltage source converter for StatCom application. Int J Emerg Electr Power Syst 8:1–6
11. Arrillaga YH, Liu NR Watson (2007) Flexible power transmission: the HVDC options. Wiley, New Jersey
12. Liu Y, Watson N, Arrillaga J (2003) A new concept for the control of the harmonic content of voltage source converters. In: The 5th international conference on power electronics and drive systems, PEDS 2003, IEEE, pp 793–798
13. Singh B, Saha R, Chandra A, Al-Haddad K (2009) Static synchronous compensators (STATCOM): a review. Power Elect IET 2:297–324
14. Norouzi AH, Sharaf A (2003) A novel control scheme for the STATCOM stability enhancement. In: Transmission and distribution conference and exposition, 2003 IEEE PES, IEEE, pp 24–29
15. Krause PC, Wasynczuk O, Sudhoff SD, Pekarek S (2013) Analysis of electric machinery and drive systems. Wiley, New Jersey
16. Han B, Choo W, Choi J, Park Y, Cho Y (2005) New configuration of 36-pulse voltage source converter using pulse-interleaving circuit. In: Proceedings of the 8th international conference on electrical machines and systems, ICEMS 2005, IEEE, pp 2389–2394
17. Liu YU, Perera LB, Arrillaga J, Watson N (2004) Harmonic reduction in the double bridge parallel converter by multi-level DC-voltage reinjection. In: 2004 international conference on power system technology 2004 PowerCon 2004, IEEE, pp 41–46
18. Voraphonpiput N, Chatratana S (2004) Analysis of quasi 24-pulse STATCOM operation and control using ATP-EMTP. In: Conference analog and digital techniques in electrical engineering
19. Valderrabano-Gonzalez A, Ramirez JM, Beltran-Carbajal F (2013) 84 pulse converter, design and simulations with Matlab
20. Valderrabano A, Ramirez JM (2010) A novel voltage source converter behind the StatCom. Elect Power Compon Syst 38:1161–1174
21. (2014) IEEE recommended practice and requirements for harmonic control in electric power systems, IEEE Std 519-2014 (Revision of IEEE Std 519-1992), pp 1–29
22. Aredes M, Santos G Jr (2000) A robust control for multipulse StatComs. In: Proceedings of IPEC, 2000, pp 2163–2168
23. Cho J-H, Song E-H (2003) Stationary reference frame-based simple active power filter with voltage regulation. In: Proceedings of industrial electronics, ISIE 2003. IEEE international symposium on IEEE 2001, pp 2044–2048
24. Mussa SA, Mohr HB (2004) Three-phase digital PLL for synchronizing on three-phase/switch/level boost rectifier by DSP. In: Power electronics specialists conference, PESC 04. IEEE 35th annual, IEEE, pp 3659–3664
25. Blazic B, Papic I (2006) Improved D-STATCOM control for operation with unbalanced currents and voltages. Power Deliv IEEE Trans 21:225–233
26. Cavaliere CA, Watanabe EH, Aredes M (2002) Multi-pulse STATCOM operation under unbalanced voltages. In: Power engineering society winter meeting, IEEE 2002, pp 567–572
27. Hochgraf C, Lasseter RH (1998) Statcom controls for operation with unbalanced voltages. Power Deliv IEEE Trans 13:538–544

28. Li K, Liu J, Wang Z, Wei B (2007) Strategies and operating point optimization of STATCOM control for voltage unbalance mitigation in three-phase three-wire systems. Power Deliv IEEE Trans 22:413–422
29. Seymour J, Horsley T (2005) The seven types of power problems. White Pap 18:1–24
30. Valderrábano A, Ramirez JM (2010) DStatCom regulation by a fuzzy segmented PI controller. Electr Power Syst Res 80:707–715
31. Pal A, Mudi R (2008) Self-tuning fuzzy PI controller and its application to HVAC systems. Int J Comput Cogn 6:25–30
32. (2009) IEEE recommended practice for monitoring electric power quality, IEEE Std 1159-2009 (Revision of IEEE Std 1159-1995), pp c1–83
33. Valderrábano-González A, Ramírez JM, Beltrán-Carbajal F (2012) Implementation of a 84-pulse voltage-source converter for special applications. IET Power Electron 5:984–990
34. Mahale P, Joshi K, Chandrakar V (2009) Static synchronous compensator (STATCOM) with Energy Storage. In: 2nd international conference on emerging trends in engineering and technology (ICETET), IEEE 2009, pp 560–563
35. Rosas-Caro JC, Ramirez JM, Peng FZ, Valderrabano A (2010) A DC-DC multilevel boost converter. Power Electron IET 3:129–137
36. Yang Z, Shen C, Zhang L, Crow M, Atcitty S (2001) Integration of a STATCOM and battery energy storage. Power Syst IEEE Trans 16:254–260
37. Zhang L, Chen S, Atcitty S, Crow M (2003) A comparison of FACTS integrated with battery energy storage systems. Institute of Electrical and Electronics Engineers, New Jersey
38. Shen D, Liu W, Wang Z (2000) Study on the operation performance of STATCOM under unbalanced and distorted system voltage. In: Power engineering society winter meeting, IEEE 2000, pp 2630–2635
39. Tsai S, Chang Y (2008) Dynamic and unbalance voltage compensation using STATCOM. In: Power and energy society general meeting-conversion and delivery of electrical energy in the 21st century, IEEE 2008, pp 1–8